Direct visualization of glutamate transporter elevator mechanism by high-speed AFM

Yi Ruan[a], Atsushi Miyagi[a,b,c], Xiaoyu Wang[b], Mohamed Chami[d], Olga Boudker[b,e,1], and Simon Scheuring[a,b,c,1]

[a]U1006 INSERM, Aix-Marseille Université, Parc Scientifique et Technologique de Luminy, 13009 Marseille, France; [b]Department of Physiology and Biophysics, Weill Cornell Medicine, New York, NY 10065; [c]Department of Anesthesiology, Weill Cornell Medicine, New York, NY 10065; [d]BioEM Lab, Center for Cellular Imaging and NanoAnalytics, Biozentrum, University of Basel, CH-4058 Basel, Switzerland; and [e]Howard Hughes Medical Institute, Weill Cornell Medicine, New York, NY 10065

Edited by Ramon Latorre, Centro Interdisciplinario de Neurociencias de Valparaíso, Facultad de Ciencias, Universidad de Valparaíso, Valparaíso, Chile, and approved December 27, 2016 (received for review October 3, 2016)

Glutamate transporters are essential for recovery of the neurotransmitter glutamate from the synaptic cleft. Crystal structures in the outward- and inward-facing conformations of a glutamate transporter homolog from archaebacterium *Pyrococcus horikoshii*, sodium/aspartate symporter Glt_{Ph}, suggested the molecular basis of the transporter cycle. However, dynamic studies of the transport mechanism have been sparse and indirect. Here we present high-speed atomic force microscopy (HS-AFM) observations of membrane-reconstituted Glt_{Ph} at work. HS-AFM movies provide unprecedented real-space and real-time visualization of the transport dynamics. Our results show transport mediated by large amplitude 1.85-nm "elevator" movements of the transport domains consistent with previous crystallographic and spectroscopic studies. Elevator dynamics occur in the absence and presence of sodium ions and aspartate, but stall in sodium alone, providing a direct visualization of the ion and substrate symport mechanism. We show unambiguously that individual protomers within the trimeric transporter function fully independently.

Glt_{Ph} | HS-AFM | transporter | elevator mechanism | dynamics

Glutamate transporters have been intensely studied, leading to elucidation of their localization, function, and structure (1–3). The major role of these transporters is to keep glutamate concentrations in the synaptic cleft below excitotoxic levels (4), and their dysfunction in the central nervous system is associated with many neurological diseases, such as epilepsy, Alzheimer's disease, and amyotrophic lateral sclerosis (5). The crystal structures of Glt_{Ph} (6, 7) provided a breakthrough in the understanding of the ion-coupled transport mechanism. The transporter forms a bowl-shaped homotrimer, in which each protomer constitutes a rigid central trimerization domain [transmembrane segments (TMs) 1, 2, 4, 5] and a peripheral transport domain (TMs 3, 6, 7, and 8, and helical hairpins 1 and 2). Aspartate (Asp) is cotransported with three sodium (Na^+) ions across the cell membrane upon a global conformational change between outward- and inward-facing states (6, 8–12). In contrast to other transporters that work by the rocker-switch (13) or the gated-pore (14) mechanisms, Glt_{Ph} mediates transport by an elevator (6) mechanism in which the transport domain travels nearly 2 nm across the membrane (reviewed in ref. 15) (Fig. S1). Single-molecule FRET (sm-FRET) experiments revealed Glt_{Ph} transport dynamics in detergent and tethered vesicles (8, 16, 17). However, direct visualization of Glt_{Ph} elevator transport mechanism remained elusive.

Results

High-speed atomic force microscopy (HS-AFM) (18) is advantageous because it probes membrane proteins in native-like lipid membranes. Thus, purified Glt_{Ph} was reconstituted into lipid mixtures yielding densely packed vesicles with diameter of up to 500 nm (Fig. S2), which opened on the HS-AFM support. First imaged under substrate-free (apo) conditions, the Glt_{Ph} trimers were well discernible in the membrane (Fig. 1*A* and Movies S1 and S2). The protomers formed protrusions of ∼2 nm in diameter and 2 nm in height with their centers separated by ∼5.5 nm. The protrusions formed triangles with a cavity at the threefold symmetry axis. These features are in agreement with the expected molecular surface of Glt_{Ph} with individual transport domains exposing their extracellular sides toward the HS-AFM tip (Fig. S3 *A* and *B*). The transport domains reversibly assumed two well-distinguishable conformations: outward facing (up, U) and inward facing (down, D) (Fig. 1*B*). The trimeric structure of the transporter was only discernible to the eye in frames where all three subunits were in the outward-facing (up) state with the transport domains protruding sharply from the membrane plane (Fig. 1*A*, many molecules; Fig. 1*B*, $t = 56$ s, $t = 57$ s).

From HS-AFM movies, we calculated kymographs of the single-transport domain dynamics (Fig. 1*C*). The domains displayed up-and-down elevator motions with an amplitude of 1.85 ± 0.42 nm (Fig. 1*D*, *Upper*), consistent with crystal structures of extreme states (Fig. S3*A*) (6, 7), sm-FRET (8, 16, 17), and electron paramagnetic resonance (EPR) (19, 20) studies. Kymographs converted to idealized traces of transitions between outward- and inward-facing conformations (Fig. 1*D*, *Lower*, and Movie S3) were used to determine the dwell times of each state.

Trimers inserted into the membrane with the intracellular side facing the HS-AFM tip were also observed (∼10%) and revealed motions (Fig. S4 and Movie S4). However, their much less pronounced surface features (Fig. S3*C*) precluded quantitative analysis.

Because the time resolution of our recordings (1 s) is comparable to the observed dwell times, we confirmed that results were not affected by faster scanning velocities (Fig. S5). The signal-to-noise ratio in measurements of small-domain movements of the Glt_{Ph} protein was diminished, and we did not use faster velocities in our further experiments.

Significance

Glutamate transporters play a crucial role for the recovery of the neurotransmitter glutamate from the synaptic cleft. Thus far, studies of the transport dynamics and detailed information of the working mechanism of this family of transmembrane proteins have been sparse and indirect. Here, we used high-speed atomic force microscopy (HS-AFM) to characterize the transport mechanisms and dynamics of a prokaryotic glutamate transporter homolog Glt_{Ph} in lipid membranes. We assess transport dynamics as a function of substrate in the imaging buffer and provide direct visual evidence that Glt_{Ph} transport domains within the trimer are entirely independent.

Author contributions: O.B. and S.S. designed research; Y.R., A.M., X.W., M.C., and S.S. performed research; Y.R. and S.S. analyzed data; and Y.R., O.B., and S.S. wrote the paper.

The authors declare no conflict of interest.

This article is a PNAS Direct Submission.

[1]To whom correspondence may be addressed. Email: sis2019@med.cornell.edu or olb2003@med.cornell.edu.

This article contains supporting information online at www.pnas.org/lookup/suppl/doi:10.1073/pnas.1616413114/-/DCSupplemental.

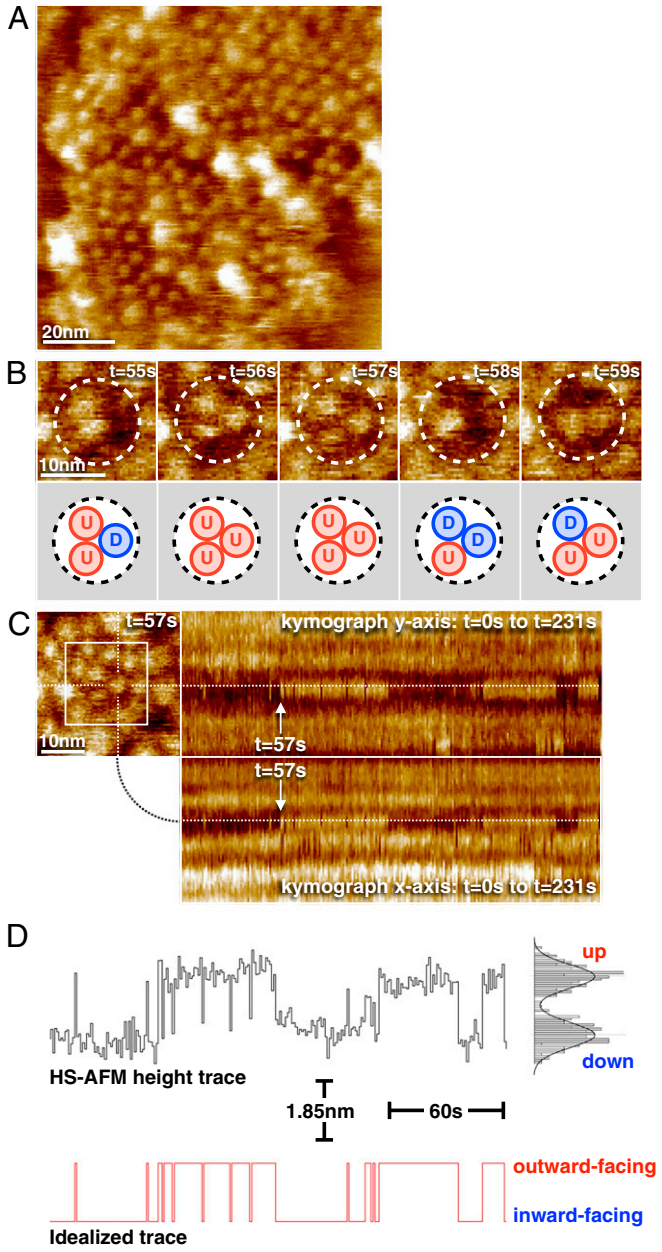

Fig. 1. Direct visualization of Glt_{Ph} elevator domain movements by HS-AFM. (*A*) A frame from a typical HS-AFM movie of a membrane containing densely packed Glt_{Ph} trimers. Full color scale is 8 nm. (*B*) Sequential frames displaying the conformational dynamics of a Glt_{Ph} trimer under substrate-free (apo) conditions. The trimer structure is only discernible to the eye in frames where all three subunits are outward facing (U, $t = 56$ s, $t = 57$ s). (*C*, *Upper Left*) Frame $t = 57$ s from image series shown in *B* (white square). (*C*, *Right*) Kymographs of the Y (*Upper*) and X (*Lower*) section profiles across a transport domain (dashed lines). Transition from down to up position at approximately $t = 57$ s is highlighted in the kymographs. Full color scale in *B* and *C* is 3 nm. (*D*, *Upper*) Height trace (average from the X and Y kymographs) as a function of time, and height value distribution histogram (*Right*). (*D*, *Lower*) Idealized trace following assignment of up and down states to outward- and inward-facing Glt_{Ph} elevator domain conformations, respectively.

Dynamic Basis of Sodium and Aspartate Symport. To correlate molecular motions to function, we first examined the dynamics of the apo Glt_{Ph} transporter under substrate-free conditions (Movie S5). HS-AFM imaging revealed frequent elevator domain movements between "up" and "down" states with dwell times of $\tau_{(up\text{-}apo)} = 6.6$ s and $\tau_{(down\text{-}apo)} = 1.8$ s (Fig. 2*A* and Table S1). Notably, only 27% of the molecules [$Q_{(apo)}$] displayed motions, whereas the rest remained inactive during the observation time windows; typical HS-AFM movie durations were ∼100 s.

As a Na^+/Asp symporter, Glt_{Ph} is expected to bind Na^+ ions with the dissociation constant of ∼100 mM (21), but not to translocate them in the absence of Asp. Consistently, we observed a dramatic decrease in the fraction of moving protomers, $Q_{(Na^+)} = 5\%$, in the presence of 1 M Na^+ only. Moreover, those molecules that exhibited movements showed a much longer average dwell time in the outward-facing state, $\tau_{(up\text{-}Na^+)} = 33.0$ s (Fig. 2*B*). Thus, Glt_{Ph} protomers bound only to Na^+ ions are mostly unable to translocate. The rare elevator motions detected are likely due to Na^+ transiently dissociating from Glt_{Ph}. Indeed, we estimate that the fraction of Na^+-free protomers is ∼3% (assuming a binding Hill coefficient of ∼1.5 as previously reported) (21) in 1 M Na^+. Interestingly, the inward-facing state remained short-lived with

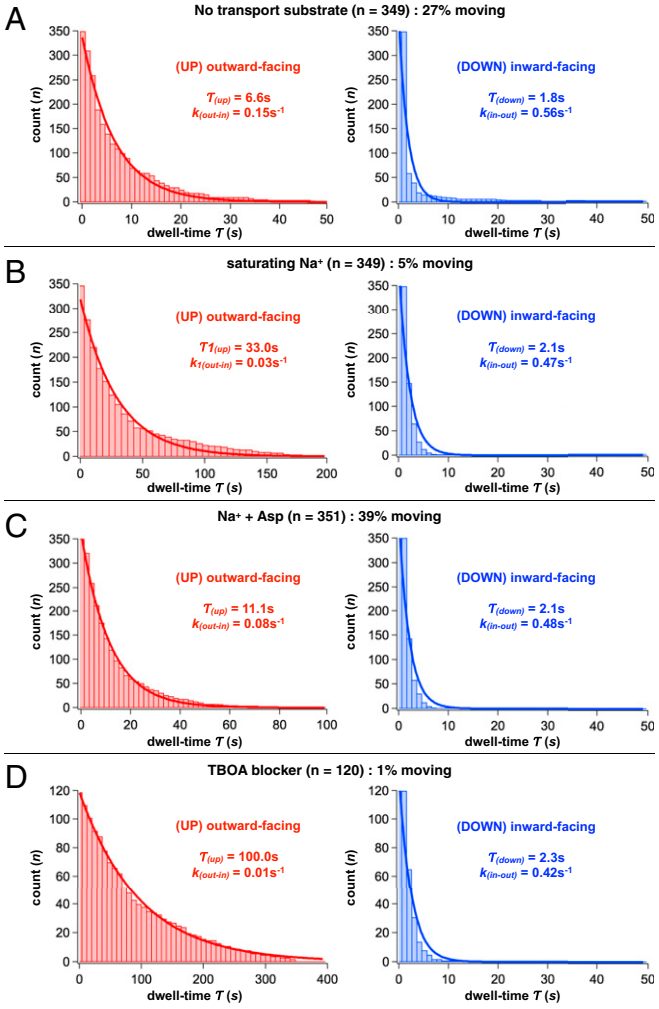

Fig. 2. Quantification of the elevator domain dynamics. Survival plots of outward-facing (*Left*, red) and inward-facing (*Right*, blue) states of the transport domain in (*A*) the absence of substrates [$\tau_{(up\text{-}apo)} = 6.6 \pm 0.3$ s; $\tau_{(down\text{-}apo)} = 1.8 \pm 0.4$ s], (*B*) the presence of saturating Na^+ [$\tau_{(up\text{-}Na^+)} = 33.0 \pm 2.1$ s; $\tau_{(down\text{-}Na^+)} = 2.1 \pm 0.3$ s], (*C*) the presence of Na^+ and aspartate [$\tau_{(up\text{-}transport)} = 11.1 \pm 0.4$ s; $\tau_{(down\text{-}transport)} = 2.1 \pm 0.3$ s], and (*D*) the presence of a nontransportable aspartate analog, DL-TBOA [$\tau_{(up\text{-}TBOA)} = 100.0 \pm 2.5$ s; $\tau_{(down\text{-}TBOA)} = 2.3 \pm 0.3$ s]. All results are given as fit parameter of $\tau \pm$ coefficient confidence interval, at 95% confidence level. The number of dynamic events analyzed, *n*, and the fractions of total protomers displaying dynamics in percentage are shown above the panels. Survival plots were fitted to single exponentials (solid lines) and corresponding lifetimes and kinetic constants are shown in the panels.

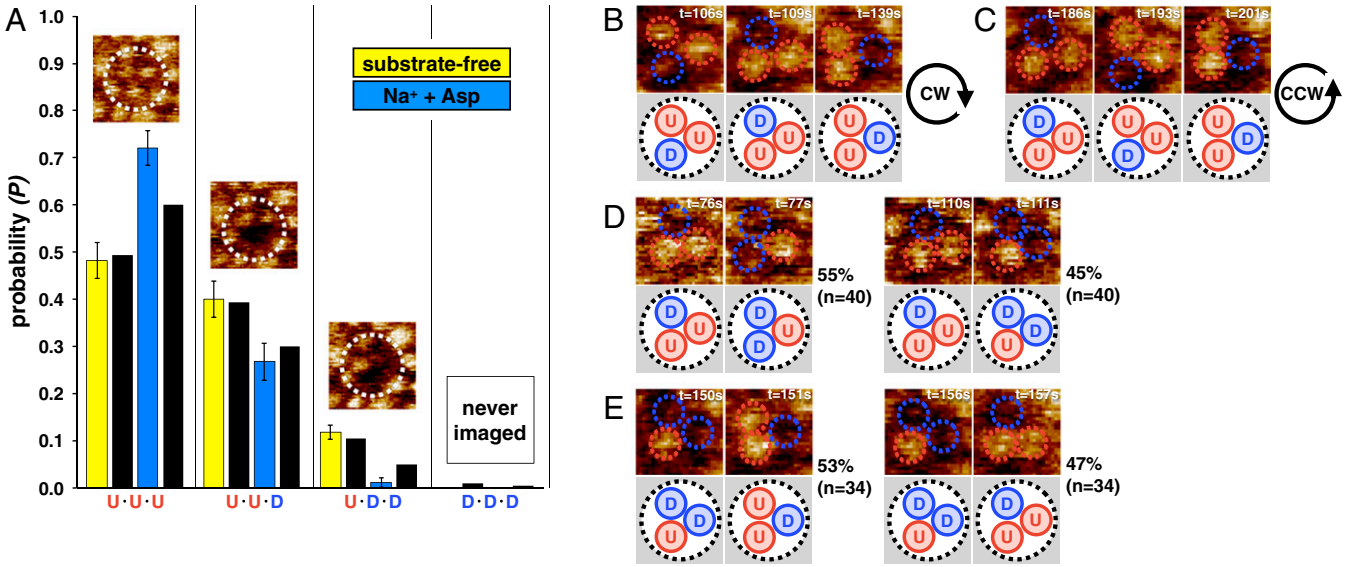

Fig. 3. Lack of cooperativity between elevator domains within Glt_{Ph} trimers. (*A*) Experimentally determined probabilities of U·U·U, U·U·D, U·D·D, and D·D·D configurations for the substrate-free (yellow) and transport (blue) conditions (n = 40 molecules). The black columns next to the experimental data represent probabilities calculated for a system of three independent protomers (Table S1). (*Insets*) Representative images of single molecules; full color scale is 3 nm. (*B–E*) Lack of order in the movements of transport domains. In trimers where single transport domains were observed to move inward one at a time, both clockwise (CW) (*B*) and counterclockwise (CCW) (*C*) orders were observed. (*D*) In trimers with one domain already in the inward-facing state, neighboring CCW (*Left*) and CW (*Right*) transport domains were equally likely to translocate from outward to inward state. (*E*) In trimers with two domains in the inward position, the probabilities that either would return to the outward position were similar. Data for *B–E* were from the recordings under transport conditions.

$\tau_{(down\text{-}Na^+)}$ = 2.1 s (Fig. 2*B*), similar to that observed in the substrate-free experiment.

We next examined the dynamics in the presence of highly saturating substrate concentrations (150 mM NaCl and 1 μM Asp). We note that the membrane-reconstituted proteins adsorbed to the HS-AFM support may experience somewhat asymmetric conditions. However, the solvent cleft between the membrane and mica is >1 nm, because proteins in less dense reconstitutions are diffusing and hence not directly interacting with the mica (22), and the trimerization domain that protrudes ∼1 nm from the membrane further elevates the membrane surface from the mica; hence, this should allow for rapid diffusion of Na^+ and Asp to the support-facing side of the membrane. Thus, we believe that the concentrations of Na^+ ions and Asp, as seen by the transporter, are the same on the opposite sides of the membrane. Glt_{Ph} shows highly cooperative and tight binding of Na^+ ions and Asp from both the extracellular and intracellular sides of the membrane (21). Under our conditions, we expect the apparent dissociation constants for Na^+ and Asp to be below 10 mM and 1 nM, respectively. Thus, the overwhelming majority of Glt_{Ph} protomers are bound to the substrates, and we must be observing bidirectional transport in our HS-AFM experiments. In contrast to Na^+ alone, the Glt_{Ph} protein showed robust dynamics when bound to both Na^+ ions and Asp with dwell times in the outward- and inward-facing conformations of, respectively, $\tau_{(up\text{-}transport)}$ = 11.1 s and $\tau_{(down\text{-}transport)}$ = 2.1 s (Fig. 2*C* and Movie S6). The population of active molecules $Q_{(transport)}$ = 39% surpassed that of the apo protein (Table S1).

In contrast, when we replaced Asp with a competitive transport blocker DL-*threo*-β-benzyloxyaspartate (DL-TBOA) (23), Glt_{Ph} remained stalled in the outward-facing state with $Q_{(TBOA)}$ = 1%, and the few observed movements occurred after long outward-facing dwells $\tau_{(up\text{-}TBOA)}$ = 100.0 s (Fig. 2*D*). On the rare occasions that an elevator domain went into the inward-facing state, $\tau_{(down\text{-}TBOA)}$ = 2.3 s was again similar to other experiments.

Collectively, HS-AFM reveals that Glt_{Ph} is much more dynamic in the absence and presence of Na^+ and Asp than when only Na^+ is present or when blocker replaces Asp. These features are in excellent agreement with what is expected for a Na^+/Asp symporter.

Glt_{Ph} Transport Domains Function Independently. HS-AFM has a unique advantage of imaging molecules directly at high spatiotemporal resolution, allowing us to analyze correlations between movements of domains within a trimer. A Glt_{Ph} trimer can adopt eight configurations with each transport domain in either outward- or inward-facing position. The populations of states with 3, 2, 1, or 0 transport domains exposed to the exterior are assessed from the experimental data (Fig. 3*A*) and agree very well with predictions based on a noncooperative

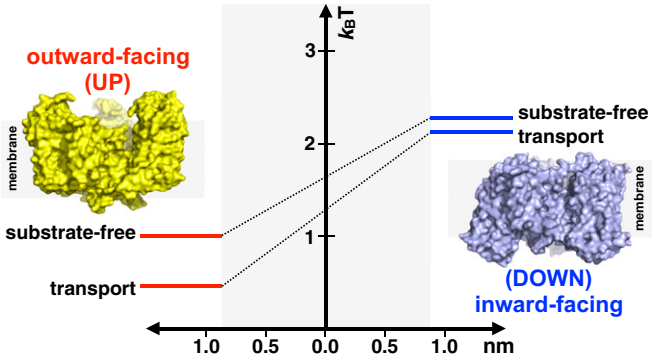

Fig. 4. Glt_{Ph} activation and movement energy landscape. An activation energy term $\Delta G_{(activation)}$ and an energy difference between the outward- and inward-facing states $\Delta G_{(translation)}$ are calculated from the fraction of active protomers and the lifetimes, respectively, for the apo and transport conditions analyzed. Note that an energy barrier higher than the inward-facing state that cannot be estimated must exist between the two states. Surface-rendered structures of the outward-facing (PDB ID code 2NWX, yellow) and the inward-facing (PDB ID code 3KBC, blue) states are shown. The gray-shaded area represents the 1.85-nm movement amplitude traveled along the reaction coordinate by the transport domain between the outward- and inward-facing states.

model (Table S2). We further detect no regularity as to whether the neighbor located clockwise or anticlockwise relative to an active elevator domain would move next: U-D-U through U-U-D to D-U-U (Fig. 3*B*), or in a counterclockwise manner from U-D-U through D-U-U to U-U-D (Fig. 3*C*). Furthermore, of 40 observations made in 6 trimers where one transport domain was already in the down position, U-D-U configuration, and a second followed, transitions into D-D-U and U-D-D configurations were observed, respectively, 22 and 18 times (Fig. 3*D*). Similarly, among 34 observations in 7 trimers where D-U-D configuration was observed, we recorded 18 and 16 transitions into U-U-D and D-U-U configurations, respectively (Fig. 3*E*). Thus, there are no correlations between the motions of individual transport domains in the Glt_{Ph} trimer. Therefore, we demonstrate unambiguously that protomers in the trimer act independently of each other in agreement with a long history of functional studies (24–26).

Energy Landscape of Transport Domain Motions. Our HS-AFM recordings provide spatiotemporal resolution that is sufficiently high and consistent to allow not only qualitative observations of domain movements, but also their quantitative analysis. Thus, we observed that the outward-facing state lifetimes and the fraction of active molecules depended on substrate binding (Table S1). Notably, the majority of molecules remain inactive during HS-AFM movie acquisition under all conditions. The reason for this inactivity remains unclear. Some molecules might be damaged, or tight protein packing might be restrictive to motions. However, the fraction of active molecules varies depending on the ligands bound to the transporter, arguing against these explanations. Alternatively, temporary inactivity could be an innate feature of the transporter; if so, it might be reminiscent of dynamic heterogeneity observed in sm-FRET studies of Glt_{Ph}, where periods of activity were interspersed by long quiescent periods (8, 16) [although not in another (17)]. Assuming that the stalled molecules observed in HS-AFM experiments reflect the reversible entry into such postulated "locked" states, we interpret the Q value (Table S1) as a fraction of unlocked active transporters. From Q values we estimate the free energy of unlocking or activation, and from the dwell times measured for the outward- and inward-facing states of the active molecules we obtain the energy difference between these states (Table S1). Notably, the outward-facing state is longer lived in the substrate-bound compared with the apo transporter. Reduced dynamics of the substrate-bound transport domain has also been observed in sm-FRET studies (8, 16). At present, we do not know why the dynamics are reduced, but we note that substrate binding is associated with minor conformational changes (10) and changes in the overall charge of the transport domain. Together, these values yield an energy landscape describing elevator domain activation and transmembrane motion (Fig. 4). These profiles are incomplete because the heights of the barriers between the states cannot be unambiguously calculated from the kinetic rates. Nevertheless, under the apo and transport conditions, the domain activation costs ~1 k_BT. Bringing the substrate-loaded domain across the membrane is associated with a slightly higher energy cost of 0.4 k_BT compared with the substrate-free domain.

Discussion

In our experiments, the inward-facing state is a short-lived, relatively high-energy state with dwell times of ~2 s under all conditions. In that regard, we do not recapitulate results of sm-FRET experiments, showing increased lifetimes of both the outward- and inward-facing states when bound to substrates (8). It cannot be excluded that the energy delivered by the HS-AFM tip speeds up inward-to-outward state transition. It is also possible that the supported membrane, which is separated from the mica support by a thin (~1 nm) cleft, biases state energies. However, it is notable that the relatively high energy of the inward-facing state combined with subunit independence would ensure that Glt_{Ph} displays probabilities of 89% in substrate-free conditions and 95% in transport conditions of having no more than one domain in the inward-facing state at a time (Fig. 3*A*). The states with multiple protomers facing inward are avoided, perhaps because in such trimers the central trimerization domain could move outward instead of the lipid-facing transport domains moving inward, making substrate transport inefficient.

In conclusion, we present real-space and real-time movies of individual transmembrane transporters at work. The unique advantage of HS-AFM is that it provides direct medium-resolution (~1 nm lateral and ~0.1 nm vertical resolution) structural and dynamic information on membrane-embedded proteins, requiring neither labeling nor complex data interpretation. Glt_{Ph}, which originates from a thermophilic prokaryote, is an exceptionally favorable model system, yet future research calls for the studies of human glutamate transporters that show much faster uptake kinetics; their turnover times range from milliseconds to just under a second for different subtypes. Our current state-of-the-art HS-AFM can reach scanning speed of 20 ms per frame when the imaging area is reduced, and pixel sampling and tip velocity are kept constant (27). However, if we were to acquire single scan lines of membrane-embedded transporters, we could generate height profiles changes with submillisecond time resolution. Ultimately, the positional readout of the cantilever reaches the microsecond regime and should allow the characterization of even faster conformational changes.

ACKNOWLEDGMENTS. We thank Dr. G. Verdon for initial protein preparation, Dr. C. M. Nimigean for advice with statistical analysis of the trimer states, and Dr. S. Blanchard for fruitful discussions. This work was supported by Agence National pour la Recherche (ANR) Grants ANR-11-IDEX-0001-02 (A*MIDEX) and ANR-Nano Grant ANR-12-BS10-009-01; European Research Council Starting Grant 310080 (to S.S.); and NIH Grant R37NS085318 (to O.B.).

1. Danbolt NC (2001) Glutamate uptake. *Prog Neurobiol* 65(1):1–105.
2. Vandenberg RJ, Ryan RM (2013) Mechanisms of glutamate transport. *Physiol Rev* 93(4):1621–1657.
3. Tzingounis AV, Wadiche JI (2007) Glutamate transporters: Confining runaway excitation by shaping synaptic transmission. *Nat Rev Neurosci* 8(12):935–947.
4. Zerangue N, Kavanaugh MP (1996) Flux coupling in a neuronal glutamate transporter. *Nature* 383(6601):634–637.
5. Takahashi K, Foster JB, Lin CL (2015) Glutamate transporter EAAT2: Regulation, function, and potential as a therapeutic target for neurological and psychiatric disease. *Cell Mol Life Sci* 72(18):3489–3506.
6. Reyes N, Ginter C, Boudker O (2009) Transport mechanism of a bacterial homologue of glutamate transporters. *Nature* 462(7275):880–885.
7. Yernool D, Boudker O, Jin Y, Gouaux E (2004) Structure of a glutamate transporter homologue from *Pyrococcus horikoshii*. *Nature* 431(7010):811–818.
8. Akyuz N, Altman RB, Blanchard SC, Boudker O (2013) Transport dynamics in a glutamate transporter homologue. *Nature* 502(7469):114–118.
9. Groeneveld M, Slotboom DJ (2010) Na(+):aspartate coupling stoichiometry in the glutamate transporter homologue Glt(Ph). *Biochemistry* 49(17):3511–3513.
10. Verdon G, Oh S, Serio RN, Boudker O (2014) Coupled ion binding and structural transitions along the transport cycle of glutamate transporters. *eLife* 3:e02283.
11. Verdon G, Boudker O (2012) Crystal structure of an asymmetric trimer of a bacterial glutamate transporter homolog. *Nat Struct Mol Biol* 19(3):355–357.
12. Boudker O, Ryan RM, Yernool D, Shimamoto K, Gouaux E (2007) Coupling substrate and ion binding to extracellular gate of a sodium-dependent aspartate transporter. *Nature* 445(7126):387–393.
13. Abramson J, et al. (2003) Structure and mechanism of the lactose permease of *Escherichia coli*. *Science* 301(5633):610–615.
14. Krishnamurthy H, Gouaux E (2012) X-ray structures of LeuT in substrate-free outward-open and apo inward-open states. *Nature* 481(7382):469–474.
15. Slotboom DJ (2014) Structural and mechanistic insights into prokaryotic energy-coupling factor transporters. *Nat Rev Microbiol* 12(2):79–87.
16. Akyuz N, et al. (2015) Transport domain unlocking sets the uptake rate of an aspartate transporter. *Nature* 518(7537):68–73.
17. Erkens GB, Hänelt I, Goudsmits JM, Slotboom DJ, van Oijen AM (2013) Unsynchronised subunit motion in single trimeric sodium-coupled aspartate transporters. *Nature* 502(7469):119–123.

18. Ando T, Uchihashi T, Scheuring S (2014) Filming biomolecular processes by high-speed atomic force microscopy. *Chem Rev* 114(6):3120–3188.
19. Hänelt I, Wunnicke D, Bordignon E, Steinhoff H-J, Slotboom DJ (2013) Conformational heterogeneity of the aspartate transporter Glt(Ph). *Nat Struct Mol Biol* 20(2):210–214.
20. Georgieva ER, Borbat PP, Ginter C, Freed JH, Boudker O (2013) Conformational ensemble of the sodium-coupled aspartate transporter. *Nat Struct Mol Biol* 20(2):215–221.
21. Reyes N, Oh S, Boudker O (2013) Binding thermodynamics of a glutamate transporter homolog. *Nat Struct Mol Biol* 20(5):634–640.
22. Casuso I, et al. (2012) Characterization of the motion of membrane proteins using high-speed atomic force microscopy. *Nat Nanotechnol* 7(8):525–529.
23. Shimamoto K, et al. (1998) DL-threo-beta-benzyloxyaspartate, a potent blocker of excitatory amino acid transporters. *Mol Pharmacol* 53(2):195–201.
24. Koch HP, Larsson HP (2005) Small-scale molecular motions accomplish glutamate uptake in human glutamate transporters. *J Neurosci* 25(7):1730–1736.
25. Grewer C, et al. (2005) Individual subunits of the glutamate transporter EAAC1 homotrimer function independently of each other. *Biochemistry* 44(35):11913–11923.
26. Leary GP, Stone EF, Holley DC, Kavanaugh MP (2007) The glutamate and chloride permeation pathways are colocalized in individual neuronal glutamate transporter subunits. *J Neurosci* 27(11):2938–2942.
27. Miyagi A, Chipot C, Rangl M, Scheuring S (2016) High-speed atomic force microscopy shows that annexin V stabilizes membranes on the second timescale. *Nat Nanotechnol* 11(9):783–790.
28. Chiaruttini N, et al. (2015) Relaxation of loaded ESCRT-III spiral springs drives membrane deformation. *Cell* 163(4):866–879.
29. Husain M, Boudier T, Paul-Gilloteaux P, Casuso I, Scheuring S (2012) Software for drift compensation, particle tracking and particle analysis of high-speed atomic force microscopy image series. *J Mol Recognit* 25(5):292–298.